THE ROLE OF ASYMPTOMATIC INFECTIONS IN THE COVID-19 EPIDEMIC VIA COMPLEX NETWORKS AND STABILITY ANALYSIS*

LEONARDO STELLA†, ALEJANDRO PINEL MARTÍNEZ†, DARIO BAUSO‡, AND PATRIZIO COLANERI§

Abstract. Italy has been the first country to be affected by the COVID-19 epidemic in Europe. In the past months, predictive mathematical models have been used to understand the proportion of this epidemic and identify effective policies to control it, but few have considered the impact of asymptomatic or paucisymptomatic infections in a structured setting. A critical problem that hinders the accuracy of these models is indeed given by the presence of a large number of asymptomatic in the population. This number is estimated to be large, sometimes between 3 and 10 times the diagnosed patients. We focus on this aspect through the formulation of a model that captures two types of interactions, one with asymptomatic individuals and another with symptomatic infected. We also extend the original model to capture the interactions in the population via complex networks, and, in particular, the Watts-Strogatz model, which is the most suitable for social networks. The contributions of this paper include: i) the formulation of an epidemic model, which we call SAIR, that discriminates between asymptomatic and symptomatic infected through different measures of interactions and the corresponding stability analysis of the system in feedback form through the calculation of the $\mathcal{R}_0$ as H_∞ gain; ii) the analysis of the corresponding structured model structure model involving the Watts and Strogatz interaction topology, to study the case of heterogeneous connectivity in the population; iii) a case study on the Italian case, where we take into account the Istat seroprevalence study in the homogeneous case first, and then we analyze the impact of summer tourism and of the start of school in September in the heterogeneous case.

Key words. COVID-19 | Complex Networks | Control Systems | Compartmental Models.

AMS subject classifications. 92D30, 93C10, 05C82.

1. Introduction.

Asymptomatic cases pose a real threat in controlling the spread of the COVID-19 disease. Recent seroprevalence studies have estimated the real number of asymptomatic individuals affected by COVID-19. Despite the surge in testing over the past months and due to a slower than expected vaccination campaign, understanding the impact of these infections in order to prevent other waves is still a crucial aspect. This work aims to study this problem and model the heterogeneous interactions in the population by means of a complex network in order to shed some light on the effectiveness of localized control measures in Italy, and to provide a better understanding of the impact of summer tourism and schools.

The model that we propose aims to capture the asymptomatic infections, or paucisymptomatic, namely individuals with one or two symptoms not including anosmia or ageusia, and the spread of latent infections. Early estimates of the transmission rate of a disease, as well as other disease parameters, play a crucial role in limiting its spread through effective policies, but subclinical cases, namely those who do not show clinical symptoms, can be misleading for an early estimate of the basic reproduction number of the disease [1]. We use official data from Protezione Civile, the

*Submitted to the editors on August 20, 2021.

†Department of Computing, College of Science & Engineering, University of Derby, Kedleston Road, DE22 1GB, United Kingdom (l.stella@derby.ac.uk, a.pinelmartinez1@unimail.derby.ac.uk).

‡Jan C. Willems Center for Systems and Control, ENTEG, Faculty of Science and Engineering, University of Groningen, The Netherlands, and with the Dipartimento di Ingegneria, University of Palermo, Italy (d.bauso@rug.nl).

§Dipartimento di Elettronica e Informazione, Politecnico di Milano, Italy (patrizio.colaneri@polimi.it).

Italian department in charge of dealing with emergencies, to fit the model, both at a national level as well as regional level. The case study provides insight on the potential effects of localized restrictions, without the coordination at a national level. The results of this study highlight the importance of coordinating the deployment of appropriate control measures that take into account the impact of asymptomatic infections, especially in younger individuals, and inter-regional movements in Italy. Previous attempts at modeling asymptomatic infections are common in the literature, for example the 2009 influenza H1N1 virus [2]. The authors in [2] discuss a model similar to the one we propose here and study the local asymptotic stability for the disease-free equilibrium and the corresponding endemic state, in presence of drug resistance. In [3], the authors consider asymptomatic infections with application to traditional models such as SIR and SEIR and to a version of the SAIR model. In that work, the main contribution is the global asymptotic stability of the SAIR model through Lyapunov stability analysis and the parameter estimation for several countries including India. The main difference with our work is that we investigate the impact of subclinical cases through two distinct measures of interactions and provide the calculation of the basic reproduction number $\mathcal{R}_0$ as the H_∞ gain.

The COVID-19 respiratory syndrome, associated with the novel strand of Coronavirus called SARS-CoV-2, has had a massive impact worldwide. Initially found in Wuhan, in the heart of Hubei Province, China [4], it has quickly spread since last December to almost every country in the world, with the most affected being the US, Spain, UK, Italy, France, Germany, Russia, Turkey, Iran, and China. This has caused severe consequences and a large number of deaths, mostly due to the ease of transmission, i.e. the virality, of this disease. For an infectious disease outbreak such as the one caused by COVID-19, predictive mathematical models play an important role for the planning of effective control strategies. Among the models formulated over the years [5, 6], the susceptible-infected-recovered model (SIR) is possibly one of the most used epidemic models: the population is split into three stages of infection, sometimes called compartments, thus the terminology *compartmental models*, as reported in an early work by Kermack and McKendrick in 1927 [7]. A variant of these classic compartmental models used to tackle the specific features of SARS can be found in the work of Gumel *et al.* [8] and similar equations can be found in the framework developed for the HIV transmission in heterogeneous populations [9]. In view of different strands of SARS-CoV-2, namely the East Asian one and the European one [10], the framework developed by Liu *et al.* can provide useful insight on the way in which two competing viruses spread in from a control perspective [11].

Several aspects of this virus have been investigated: some research assessed the effectiveness of different response strategies [12], another study focused on modeling the various stages of the disease and the death rate in response to population-wide interventions *et al.* [13], recently extended to include vaccination rollout and non-pharmaceutical interventions (NPIs) in Italy [14]. Early research in China showed unique epidemiological traits of the COVID-19 virus [15], most notably the fact that a large portion of transmissions were caused by asymptomatic individuals, whether they were showing mild or no symptoms at all. Indeed, further research demonstrated that asymptomatic and symptomatic individuals have the same viral load and thus the same capability to further spread the virus [16], and the work of Rothe *et al.* provides evidence for transmission from an asymptomatic individual in Germany [17]. In the context of data driven models, Bertozzi *et al.* find a relation between branching point processes and classical compartmental models such as susceptible-infected-recovered (SIR) and susceptible-exposed-infected-recovered (SEIR), whilst fitting the models

with data from a variety of countries, including China, Italy, Japan, and other countries [18]. A study that investigates whether daily test reports can help authorities to control the epidemic [19], discusses how mitigation strategies can fail when modelled because of various factors, such as delay, unstable dynamics, and uncertainty in the feedback loop. For the Italian situation, the work of Della Rossa *et al.* provides interesting insight on the need to coordinate the efforts in controlling the situations in an inter-regional setting, and highlights the need of such coordination by means of a network model [20]. In the work of Yilmaz *et al.*, the authors discuss how to identify and analyze bridges between communities in graphs with the purpose to understand how to track and where to start tests on which individuals [21]. Another study includes a particle-based mean field model that investigates the pros and cons of social distancing through an approach that compares individuals to molecules in a chemical solution [22]. A very early model of this disease was given in the work by Calafiore *et al.*, where the novelty lies in including a proportionality factor in a standard SIR model to account for hidden infections [23]. In a model on the case for the UK, the authors account for four main elements and a finer level of detail for each of them in assessing the impact of the speed in which the immunity is lost [24]. A risk sensitivity analysis is conducted on the economic impact of the disease where the optimizing behavior of agents to influence future transitions is considered by Garibaldi *et al.* [25]. The work by Pastor-Satorras provides a survey of the literature on complex networks for epidemic processes [26], and applications of complex networks to epidemic processes in evolutionary dynamics can be found in the work by Tan *et al.* [27]. Finally, in [28], the authors study the equilibria, stability and convergence of classical virus propagation models. Of specific interest for our study is their analysis of the SIR model over contact networks with a strongly-connected topology, whereas we focus on heterogeneous connectivity via complex networks. Another difference with our work is the investigation of the epidemic outbreak in relation to our parameters of infections to establish a threshold in relation to the epidemic outbreak.

Highlights of contributions. We propose an epidemic predictive model that discriminates between asymptomatic and symptomatic cases of COVID-19 through two different measures of connectivity, as interactions with these two classes are captured separately, allowing for a study on the impact of asymptomatic cases. The main reason as to discuss this model in place of the well-known SEIR model is twofold: first, a distinctive feature of COVID-19 is the presence of a large number of asymptomatic infected; second, unlike the traditional SEIR model, the asymptomatic class can infect and indeed is responsible for the vast majority of infections in line with the ones reported for COVID-19. By rewriting the proposed model in feedback form we study the equilibrium and convergence via the calculation of the basic reproduction number $\mathcal{R}_0$ as the H_∞ gain. We extend the model to consider heterogeneous connectivity in the form of the Watts-Strogatz complex network, which is commonly used to model social interactions because of its small world property. The stability and convergence analysis of this model is carried out in an analogous manner to the homogeneous case. Finally, a case study on the situation in Italy is given: first, the homogeneous model is used to compare the official data with the data of the recent seroprevalence study from Istat; second, in view of the return to school in mid-September and the diverse impact of tourism across the regions, a study at regional level is conducted. The results emphasize the need for coordinated control measures that account for the interactions among different regions in Italy, or in general different countries.

Relevance of this work. This work is one of the first attempts to use the Istat seroprevalence study to model the evolution of SARS-CoV-2 at national level and by

making use of complex networks to model the inter-regional spread of the virus for the situation in Italy. This work develops a predictive model which highlights the impact of asymptomatic infections in spreading the disease through two different measures of their interactions. The analysis of the possible scenarios following the return to schools in mid-September 2020 is carried out via heterogeneous connectivity in the population by means of a complex network. Finally, a case study for the Italian case confirms that only centralized coordinated policy decisions at national level can be effective when inter-regional movements are allowed.

The paper is organized as follows. In Section 2, we discuss the main results of our work when the population is homogeneous and carry out the stability analysis of our model. Section 3 extends the previous results to a structured model, where the structure is captured by a complex network. In Section 4, we provide a numerical analysis and discuss our algorithm to estimate the parameters of the homogeneous model, while the main case studies are discussed in Section 5. Finally, in Section 6 conclusions are drawn and future research is discussed.

2. Homogeneous Epidemic Model. In this section, we present the formulation of the model that we propose, which takes inspiration from popular compartmental models such as the widely used susceptible-infected-recovered (SIR) model, and more precisely from the susceptible-exposed-infected-recovered (SEIR) model. In a compartmental model, the population is divided into a discrete set of states, or compartments. For instance, in the SIR model, individuals can be susceptible to the virus, then get infected, and finally recover or pass away. The SIR model accounts for those diseases that do provide long term immunity to future infections from the same virus through the presence of antibodies in the host organism, but other models, e.g. the SIS model, consider the possibility of re-infections.

In line with previous works [2, 3], we named the model *SAIR*, because of the state variables we chose to include: Susceptible, Asymptomatic infected, symptomatic Infected and Removed. We choose to use the term *removed* in place of the more common *recovered* because we do not discriminate between individuals that recover from the disease and those that pass away. The term *removed* is also used commonly in the literature, see e.g. [29]. As previously mentioned, our model is a variation of the susceptible-exposed-infected-recovered (SEIR) [30], but with notable differences:

- Our (A)symptomatic class captures the infections in the population with little or no symptoms. After a while, asymptomatic infected can show symptoms or recover from the virus, which is usually different from the traditional Markov chain associated with the SEIR model (Exposed usually need to become Infected first). Furthermore, infections spread by asymptomatic individuals are possible and indeed are common, in line with what reported for COVID-19.
- Our study focuses on the impact of the undetected asymptomatic individuals in spreading the virus. Some of these can show symptoms at a later stage, and we assume that in an initial stage no individuals show symptoms. The susceptible individuals can interact with asymptomatic or symptomatic infected and become asymptomatic first. In the model this is done through different parameters of infection and two separate measures of connectivity.

In the rest of the paper, we provide an estimation of the parameters of infection through a case study for Italy. We estimate the ratio between asymptomatic and symptomatic infected and support our work with the estimate from the Istat seroprevalence study [31]. We then investigate the impact of the lockdown measures in controlling the spread of the virus, by modelling the frequency of contacts among

the individuals in the population via an average number of contacts, first, and then through the small-world complex network model.

The susceptible-asymptomatic-infected-removed (SAIR) model that we present in the following is a discrete-state continuous-time system. In a first approximation, individuals are considered homogeneous, namely they share the same properties when in the same state (or compartment). The state variables of the model represent the densities of susceptible, asymptomatic infected, symptomatic infected and removed individuals. These quantities are denoted by $S(t)$, $A(t)$, $I(t)$ and $R(t)$, respectively. Each state variable belongs to $\mathbb{R}_0^+$. In the mean-field limit, the following system of ODEs describes the time evolution of the population:

$$\begin{cases} \dot{S}(t) = -S(t)(\bar{k}_1\gamma A(t) + \bar{k}_2\lambda I(t)), \\ \dot{A}(t) = S(t)(\bar{k}_1\gamma A(t) + \bar{k}_2\lambda I(t)) - A(t)(\alpha + \sigma), \\ \dot{I}(t) = \alpha A(t) - \mu I(t), \\ \dot{R}(t) = \sigma A(t) + \mu I(t), \end{cases} \tag{2.1}$$

where the uppercase Latin letters represent the known classes, $\bar{k}_1$ and $\bar{k}_2$ take values in [0 1] and describe the amount of interactions with asymptomatic and symptomatic individuals, respectively: the lower bound represents no interactions, and the upper bound represents the situation where individuals have the normal daily interactions. These parameters can be seen as control/tuning parameters based on the NPIs at any given point in time. The lower bound represents an absence of the usual interactions in the population and the upper bound represents the daily interactions in the population without any restrictions. The lowercase Greek letters represent the parameters of the system. In particular, these parameters are constant positive quantities and have the following physical interpretation: γ and λ denote the microscopic transmission rate, the former due to contacts between a susceptible person and an asymptomatic infected, the latter due to contacts between a susceptible person and a symptomatic infected; infected individuals decay into the removed class at rate σ from the asymptomatic infected state and at rate μ from the symptomatic infected state, respectively; finally, α is the rate at which asymptomatic individuals develop symptoms.

System (2.1) is a nonlinear positive system, more precisely it is bilinear, since the highest degree that we have is at most two, obtained from the multiplication between two state variables. The fact that the system is positive means that, given an initial condition $S(0), A(0), I(0), R(0) \geq 0$, all the state variables take nonnegative values for $t \geq 0$. Furthermore, due to the conservation of mass, namely $\dot{S}(t)+\dot{A}(t)+\dot{I}(t)+\dot{R}(t) = 0$, all state variables are linked through the normalisation condition:

$$S(t) + A(t) + I(t) + R(t) = 1,$$

meaning that the sum of all the state variables is constant at any given time and equal to one.

In line with the work by Giordano *et al.* [13], the following conditions hold: $\gamma\bar{k}_1 > \lambda\bar{k}_2$, due to the fact that people are more likely in contact with, or closer to, asymptomatic infected rather than with individuals that show clear symptoms. In our model we assume the *homogeneous mixing* hypothesis [5], which asserts that the rate of infection per capita of the susceptible individuals is proportional to the number of people already infected. Because of this hypothesis, system (2.1) is treated as a mean-field model where the rate of contacts between susceptibles and both symptomatic and asymptomatic individuals is assumed constant, independently of any

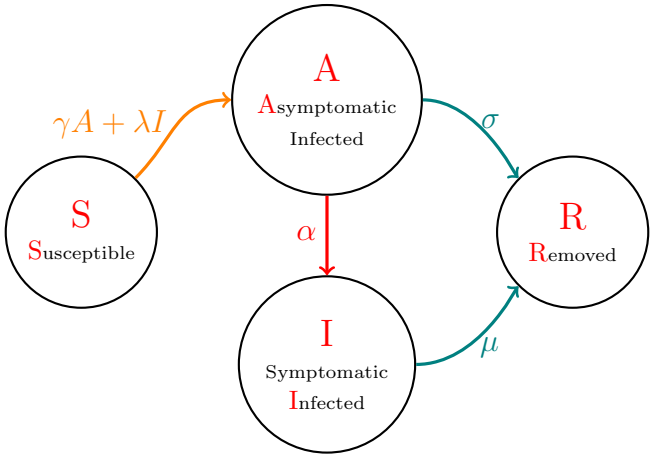

Fig. 1: Markov chain representation describing the transition rates between the states of the SAIR model in (2.1).

source of heterogeneity present in the system. Figure 1 depicts the Markov chain corresponding to system (2.1).

Let $z(t) = [S(t)\, A(t)\, I(t)\, R(t)]^\top$, system (2.1) can be rewritten in matrix form as:

$$\dot{z}(t) = G(S(t))z(t),$$

which is equivalent to

$$\underbrace{\begin{bmatrix} \dot{S} \\ \dot{A} \\ \dot{I} \\ \dot{R} \end{bmatrix}}_{\dot{z}} = \underbrace{\begin{bmatrix} 0 & -\bar{k}_1\gamma S & -\bar{k}_2\lambda S & 0 \\ 0 & \bar{k}_1\gamma S - \alpha - \sigma & \bar{k}_2\lambda S & 0 \\ 0 & \alpha & -\mu & 0 \\ 0 & \sigma & \mu & 0 \end{bmatrix}}_{G(S)} \underbrace{\begin{bmatrix} S \\ A \\ I \\ R \end{bmatrix}}_{z}, \tag{2.2}$$

where the dependence on time is implicit, e.g. $S := S(t)$, for the sake of brevity. As depicted in Fig. 2, the above system can be rewritten in feedback form, where the subsystem consisting of variables A and I can be seen as a positive linear system under feedback. Let $x(t) = [A(t)\, I(t)]^\top$, system (2.2) can be rewritten in feedback form as:

$$\dot{x}(t) = Fx(t) + bu(t), \tag{2.3}$$

$$y(t) = cx(t), \tag{2.4}$$

$$u(t) = S(t)y(t), \tag{2.5}$$

where F, b and c are defined as

$$F = \begin{bmatrix} -\alpha - \sigma & 0 \\ \alpha & -\mu \end{bmatrix}, \quad b = \begin{bmatrix} 1 \\ 0 \end{bmatrix}, \quad c = [\bar{k}_1\gamma \;\; \bar{k}_2\lambda].$$

The remaining variables satisfy the following differential equations:

$$\dot{S}(t) = -S(t)y(t) = -u(t), \tag{2.6}$$

$$\dot{R}(t) = Ex(t) = [\sigma \;\; \mu]x(t). \tag{2.7}$$

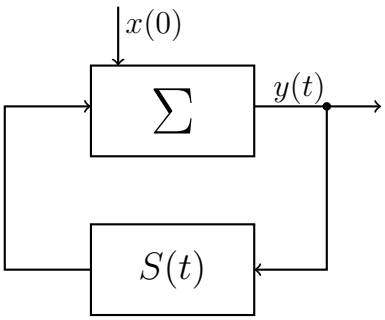

Fig. 2: The SAIR system in feedback form corresponding to equations in (2.3)-(2.5), where the subsystem indicated by Σ can be seen as a positive linear system under feedback.

LEMMA 2.1. *System (2.2) with constant parameters admits the following equilibria:* $z^* = (\bar{S}, 0, \bar{R})$, *with* $\bar{S} + \bar{R} = 1$.

Proof of Lemma 2.1. The equilibria $(\bar{S}, 0, 0, \bar{R})$, with $\bar{S} + \bar{R} = 1$, follow from either $S = 0$ or $\bar{k}_1\gamma A + \bar{k}_2\lambda I = 0$, which in turns means $A = I = 0$ (or both at the same time). In the first case, if $S = 0$, $\dot{A} = 0$ and $\dot{I} = 0$, if and only if $A = 0$ and $I = 0$, and $\dot{R} = 0$. In the second case, if $A = I = 0$, then $\dot{A} = \dot{I} = 0$ and also $\dot{R} = 0$. This concludes the proof. ■

A fundamental result on stability and convergence of the system in feedback form (2.3)-(2.5) hinges on the definition of the so-called basic reproduction number $\mathcal{R}_0$, defined as the H_∞ norm of the transfer function of the open-loop positive system (F, b, c) in (2.3)-(2.4) with constant parameters in F and c, i.e.

$$\mathcal{R}_0 = -cF^{-1}b = \frac{\bar{k}_1\gamma\mu + \bar{k}_2\lambda\alpha}{(\alpha + \sigma)\mu}.$$

The above satisfies the well-known property (inherited by standard small gain argument) that stability of the positive LTI system (2.3)-(2.5) with constant susceptible population $\bar{S}$ is equivalent to $\mathcal{R}_0\bar{S} < 1$ [13].

Remark. The basic reproduction number $\mathcal{R}_0$ is the initial value at the outbreak of the epidemic. For instance, in the case of COVID-19 in Italy it was calculated to range from 2.43 to 3.1 [32]. Parameters $\bar{k}_1 \leq 1$ and $\bar{k}_2 \leq 1$ reflect the NPIs (non-pharmaceutical interventions) such as closure of social activities, wearing masks, social distancing or in response to the vaccination campaign [14]. The well-known current reproduction number is defined as $\mathcal{R}(t) = \mathcal{R}_0 S(t)$. This parameter becomes smaller for decreasing $S(t)$. Therefore, in absence of containment measures ($\bar{k}_1 = 1$, $\bar{k}_2 = 1$), the herd immunity is reached at time $S(\bar{t})$ when $S(\bar{t}) = 1/\mathcal{R}_0$, i.e. assuming $\mathcal{R}_0 = 2.5$ for the COVID-19, $S(\bar{t}) = 0.4$, meaning that 60% of the population has been exposed to the virus and is infected, recovered, dead or immunized through vaccination.

We now study our system to assess the presence of a nonzero epidemic threshold for our model. The significance of this threshold is such that it can be used to predict the propagation of the virus at the initial stage of the epidemic. Indeed, if the value of the infection rates is greater than this threshold, the fraction of infected individual at the end of the epidemic (also called *epidemic prevalence*), namely $\bar{R} = \lim_{t\to\infty} R(t)$,

attains a finite value in a large population. However, when the value of the infection rates is below the threshold, the epidemic prevalence is infinitesimally small for large populations [29, 30]. In the following, we provide an analytic expression for this critical threshold as a function of the connectivity measures $\bar{k}_1$ and $\bar{k}_2$ and we show the connection between this value and the basic reproduction number $\mathcal{R}_0$.

Let us consider system (2.1) and, without lack of generality, set the initial conditions $R(0) = 0$ and $S(0) \simeq 1$, which implies that only a very small number of infected individuals $A(0) = I(0) \simeq 0$ is present at the start of the epidemic. The following result provides the value of the epidemic threshold ensuring $\mathcal{R}_0 > 1$ that means the rise of the infection variables and the surge of the epidemic.

THEOREM 2.2. *Consider system (2.1) with initial conditions $R(0) = 0$, $A(0) = I(0) \simeq 0$, $S(0) \simeq 1$. This system admits a nonzero epidemic prevalence if and only if*

$$\gamma > \gamma_c(1-p), \qquad \lambda > \lambda_c p,$$

for some $p \in [0\ 1]$ where γ_c and λ_c are the thresholds for the asymptomatic and symptomatic infection rates, respectively. These are defined as:

$$\gamma_c \triangleq \frac{(\alpha+\sigma)}{\bar{k}_1}, \qquad \lambda_c \triangleq \frac{(\alpha+\sigma)\mu}{\bar{k}_2\alpha}. \tag{2.8}$$

Proof of Theorem 2.2. We start by integrating the equation for $S(t)$ in system (2.1) as in the following:

$$S(t) = S(0)e^{-\int_0^t \phi(\tau)\mathrm{d}\tau},$$

where the integral is defined as

$$\int_0^t \phi(\tau)\mathrm{d}\tau = [\bar{k}_1\gamma\ \bar{k}_2\lambda] \begin{bmatrix} \alpha & -\mu \\ \sigma & \mu \end{bmatrix}^{-1} \begin{bmatrix} I(t)-I(0) \\ R(t)-R(0) \end{bmatrix}.$$

The above then yields

$$S(t) = S(0)e^{-\left(\frac{\bar{k}_1\gamma\mu-\bar{k}_2\lambda\sigma}{(\alpha+\sigma)\mu}(I(t)-I(0))+\frac{\bar{k}_1\gamma\mu+\bar{k}_2\lambda\alpha}{(\alpha+\sigma)\mu}(R(t)-R(0))\right)},$$

which can be simplified by taking into account the initial conditions, namely $S(0) \simeq 1$, $I(0) \simeq 0$ and $R(0) = 0$ as specified in the statement of the theorem, and the fact that at the end of the epidemic the number of infected is $\lim_{t\to\infty} I(t) = 0$ as in the following:

$$\bar{S} = e^{-\mathcal{R}_0\bar{R}},$$

where the total number of infected $\bar{R} = \lim_{t\to\infty} R(t)$ and $\mathcal{R}_0$ is the basic reproduction number. We can now combine the above equation with the normalization condition and we can see that the total number of infected $\bar{R}$ fulfils the following equation:

$$\bar{R} = 1 - e^{-\mathcal{R}_0\bar{R}}.$$

A trivial solution of the above equation is $\bar{R} = 0$, but we seek nonzero solutions. Notice that such solution is equivalent to the basic reproduction number

$$\mathcal{R}_0 = \frac{\mathrm{d}}{\mathrm{d}\bar{R}}\left(1 - e^{-\mathcal{R}_0\bar{R}}\right)\Big|_{\bar{R}=0}.$$

Therefore, thanks to (2.8), if $\gamma > \gamma_c(1-p)$ and $\lambda > \lambda_c p$, it turns out that the above equation is equivalent to the following:

$$\mathcal{R}_0 = \gamma\frac{\bar{k}_1}{\alpha+\sigma} + \lambda\frac{\bar{k}_2\sigma}{(\alpha+\sigma)\mu} > (1-p)+p = 1.$$

Conversely, if $\mathcal{R}_0 > 1$, there exists p for which $\gamma > \gamma_c(1-p)$ and $\lambda > \lambda_c p$. This concludes the proof. ■

In the following, we characterize the stability and convergence property of the infection stage variables, i.e. A and I, along with the susceptible and recovered classes S and R. We start by assuming that the parameters are constant after time $\bar{t}$ that is set to zero for sake of simplicity of the notation.

THEOREM 2.3. *Assume that the parameters in F and c are constant for $t \geq 0$, and $E \gg 0$. Then,*

$$\log\frac{S(0)}{S(t)} - \mathcal{R}_0(S(0)-S(t)) = \frac{\bar{k}_2\lambda}{\mu}(I(0)-I(t)) + \mathcal{R}_0(A(0)-A(t)),\ \forall t \geq 0, \tag{2.9}$$

$$\lim_{t\to\infty} A(t) = 0, \tag{2.10}$$

$$\lim_{t\to\infty} I(t) = 0, \tag{2.11}$$

$$\lim_{t\to\infty} S(t) = \bar{S} < \frac{1}{\mathcal{R}_0}, \tag{2.12}$$

where $\bar{S}$ is the only solution of

$$\log\frac{S(0)}{\bar{S}} - \mathcal{R}_0(S(0)-\bar{S}) = \frac{\bar{k}_2\lambda}{\mu}I(0) + \mathcal{R}_0 A(0). \tag{2.13}$$

Finally,

$$\bar{R} = \lim_{t\to\infty} R(t) = 1 - \bar{S}. \tag{2.14}$$

Proof of Theorem 2.3. In the following, recall that $x = [A\ I]^\top$. The equation (2.9) comes from integrating $\dot{x} = (F+bSc)x = Fx - b\dot{S}$ and taking into account that $\dot{S}/S = -cx$. Consider function $W = \mathbf{1}^\top x + S$, and take the derivative along the trajectories of system (2.2). Since $\mathbf{1}^\top F = -E \ll 0$ we have that:

$$\dot{W}(x,S) = \mathbf{1}^\top(F+bSc)x + \dot{S} = \mathbf{1}^\top(F+bSc)x - Scx = -Ex < 0, \quad x \neq 0.$$

This means that $x \to 0$, and therefore claims (2.10)-(2.11) are met, and $S \to \bar{S}$ for a nonnegative $\bar{S}$, see the characterization of the equilibrium point in Lemma 2.1. Therefore, (2.13) follows from (2.9) because of claims (2.10)-(2.11). As for the inequality in (2.12), notice that the left-hand side of (2.13) is ∞ for $\bar{S} = 0$ and 0 for $\bar{S} = S(0)$. Moreover its derivative with respect to $\bar{S}$ is $\mathcal{R}_0 - 1/\bar{S}$. The only point of intersection between the LHS and (positive) RHS of (2.13) is such that $\bar{S} < 1/\mathcal{R}_0$. This justifies the inequality in (2.12). The proof of (2.14) is trivial. ■

Remark. The above result allows us to calculate the equilibrium point of our model when the parameters in F and c are known and the initial conditions are given. This result can be extended for any $t > 0$ by using the values of the parameters in F and c and the value of each compartment at $t > 0$. Most importantly, note that formula (2.9) defines a "potential" function of the epidemic system. Indeed, the function

$$f(S,A,I) = -log(S) + \mathcal{R}_0 S + \mathcal{R}_0 A + \frac{\lambda}{\mu}\bar{k}_2 I \tag{2.15}$$

is constant along the trajectories of the system.

Due to the triangular structure of the SAIR epidemic model, the linear part $\dot{x} = Fx$ is robustly stable under uncertain time-varying parameters in F and c [33]. This property implies convergence of $A(t)$ and $I(t)$ of the nonlinear feedback system (2.3)-(2.5) to zero for any bounded time-varying parameters in F and c.

THEOREM 2.4. *Assume that the parameters in F and c are bounded time-varying parameters for $t \geq 0$. The nonlinear feedback system (2.3)-(2.5) is exponentially convergent to $\bar{A} = 0$, $\bar{I} = 0$ and some constant value $\bar{S} \geq 0$ that depends on the time-evolution of the parameters.*

Proof of Theorem 2.4. In the following, recall that $x = [A\ I]^\top$. The linear system $\dot{x} = Fx$ is robustly stable with the common copositive linear Lyapunov function $\mathbf{1}^\top x$. Then $\mathbf{1}^\top Fx = -Ex < 0$, $x \neq 0$, for any bounded time-varying parameters in F. Consider now the function

$$V(x, S) = \mathbf{1}^\top x + S.$$

Therefore,

$$\dot{V} = \mathbf{1}^\top Fx = -Ex < 0, \quad x \neq 0.$$

Therefore x converges to 0 and from $\dot{S} \leq 0$, S converges to a constant $\bar{S}$ that depends of the time-varying parameters in F and c. This concludes the proof. ∎

In the following, we focus on the impact that asymptomatic infections have on the equilibrium and stability. In order to assess this impact, we study the dynamics of the ratio between the symptomatic infected and the asymptomatic infected, namely $\tilde{I} := I/A$. We can calculate the corresponding ODE as:

$$\begin{aligned}\dot{\tilde{I}} =& \frac{\dot{I}A - I\dot{A}}{A^2} \\ =& \frac{(\alpha A - \mu I)A}{A^2} - \frac{(\bar{k}_1\gamma A + \bar{k}_2\lambda I)IS}{A^2} + \frac{(\alpha+\sigma)IA}{A^2} \\ =& \alpha - (\mu + \bar{k}_1\gamma S - \alpha - \sigma)\tilde{I} - \bar{k}_2\lambda S\tilde{I}^2,\end{aligned} \tag{2.16}$$

and therefore $\dot{\tilde{I}}$ satisfies a differential Riccati equation as

$$\dot{\tilde{I}} = \alpha - (\mu + \bar{k}_1\gamma S - \alpha - \sigma)\tilde{I} - \bar{k}_2\lambda S\tilde{I}^2, \tag{2.17}$$

where the state variables S and A can be rewritten as:

$$\begin{aligned}\dot{S} &= -SA(\bar{k}_1\gamma + \bar{k}_2\lambda\tilde{I}), \\ \dot{A} &= SA(\bar{k}_1\gamma + \bar{k}_2\lambda\tilde{I}) - A(\alpha+\sigma).\end{aligned} \tag{2.18}$$

Therefore, the equilibrium $\bar{\tilde{I}}$ of (2.17) is the stabilizing solution (max solution) of the associated algebraic Riccati equation as stated in the following theorem, reported without proof since it is straightforward.

THEOREM 2.5. *Assume that all parameters are constant. Equation (2.17) tends to the equilibrium*

$$\bar{\tilde{I}} = \frac{1}{2\bar{k}_2\lambda\bar{S}}\Big(h - \bar{k}_1\gamma\bar{S} + \sqrt{(h - \bar{k}_1\gamma\bar{S})^2 + 4\alpha\bar{k}_2\lambda\bar{S}}\Big), \tag{2.19}$$

where $h := \alpha + \sigma - \mu$, and $\bar{S}$ is the equilibrium in Theorem 2.3. Furthermore, the equilibrium $\bar{\tilde{I}}$ is asymptotically stable.

3. Heterogeneous Interaction Model. In the previous section, we have studied the model where all individuals in the population are homogeneous, namely they are indistinguishable, as they have the same value to measure the average number of contacts. In this section, we extend the previous model to address the effects of contact heterogeneity in the form of complex networks. Given a large population, let $P(k)$ be the probability distribution of the node degrees for a complex network representing the interactions of the individuals in the population. Similarly to (2.3), let $x^{[k]}(t) = [A_k(t)\ I_k(t)]^\top$ for any k-th class of connectivity, for $k = 1, \dots, N$. Let $\theta_i(t) := \frac{1}{\langle f \rangle} \sum_{k=1}^{N} n(k)P(k)x_i^{[k]}(t)$ be the probability that a randomly chosen link will point to $x_i^{[k]}(t)$, namely an asymptomatic infected for $i = 1$ for any class k, and a symptomatic infected for $i = 2$ for any class k, where $\langle f \rangle$ represents the average connectivity and is obtained from taking the mean value of the connectivity across all classes k, and the measure of connectivity $n(k)$ assigns the number of connections to each class of connectivity. Finally, let $\psi_{i,k} := n(k)/k_{i,max}$, where $k_{i,max}$ is the maximum number of contacts without restrictions. When $n(k)$ is the maximum number of contacts without restrictions, namely $n(k) = k_{i,max}$, for all classes k, we return to the homogeneous case. Parameters $\psi_{i,k}$ describe the connectivity towards the asymptomatic and symptomatic infected for $i = 1$ and $i = 2$, respectively.

Let $z_k(t) = [S_k(t)\, A_k(t)\, I_k(t)\, R_k(t)]^\top$ be the population state at time t of degree of connectivity $n(k)$. The magnitudes $S_k(t)$, $A_k(t)$, $I_k(t)$ and $R_k(t)$ represent the density of the susceptible, asymptomatic infected, symptomatic infected and removed nodes of connectivity k at time t, respectively. As before, these variables must satisfy the normalization condition for each k:

$$S_k(t) + A_k(t) + I_k(t) + R_k(t) = 1.$$

For each k, system (2.1) becomes:

$$\begin{cases} \dot{S}_k(t) = -S_k(t)(\psi_{1,k}\gamma\theta_1(t) + \psi_{2,k}\lambda\theta_2(t)), \\ \dot{A}_k(t) = S_k(t)(\psi_{1,k}\gamma\theta_1(t) + \psi_{2,k}\lambda\theta_2(t)) - A_k(t)(\alpha + \sigma), \\ \dot{I}_k(t) = \alpha A_k(t) - \mu I_k(t), \\ \dot{R}_k(t) = \sigma A_k(t) + \mu I_k(t). \end{cases} \tag{3.1}$$

Each node of the network represents an individual and their corresponding state, i.e. susceptible, asymptomatic infected, symptomatic infected and removed. In matrix form, where the dependence on time is implicit for the sake of brevity, the above system becomes:

$$\begin{bmatrix} \dot{S}_k \\ \dot{A}_k \\ \dot{I}_k \\ \dot{R}_k \end{bmatrix} = \underbrace{\begin{bmatrix} -(\psi_{1,k}\gamma\theta_1 + \psi_{2,k}\lambda\theta_2) & 0 & 0 & 0 \\ (\psi_{1,k}\gamma\theta_1 + \psi_{2,k}\lambda\theta_2) & -(\alpha+\sigma) & 0 & 0 \\ 0 & \alpha & -\mu & 0 \\ 0 & \sigma & \mu & 0 \end{bmatrix}}_{G_k(\theta)} \begin{bmatrix} S_k \\ A_k \\ I_k \\ R_k \end{bmatrix}, \tag{3.2}$$

where $\theta := [\theta_1\, \theta_2]^\top$ is a function of the infection states as defined above and $G_k(\theta)$ depends explicitly on the measure of connectivity $n(k)$ and on θ.

As for the homogeneous case, we can rewrite the above system in feedback form. We start by writing each system corresponding to the degree of connectivity $n(k)$ and then we write the whole system comprising all $k \in [1\ N]$. Let $x^{[k]}(t) = [A_k(t)\ I_k(t)]^\top$,

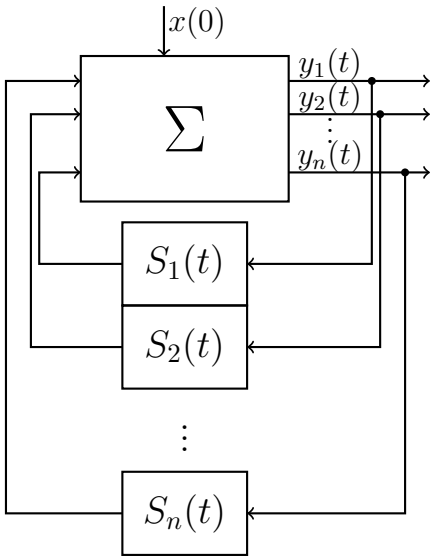

Fig. 3: The heterogeneous SAIR system in feedback form corresponding to equations (3.3)-(3.5).

system (3.2) in feedback form is the following:

$$\dot{x}^{[k]}(t) = Fx^{[k]}(t) + bu_k(t), \tag{3.3}$$

$$y_k(t) = c_k \sum_{j=1}^{N} n(j)P(j)x^{[j]}(t), \tag{3.4}$$

$$u_k(t) = S_k(t)y_k(t), \tag{3.5}$$

where F and b are defined as in the homogeneous case and c_k is:

$$c_k = \begin{bmatrix} \dfrac{\psi_{1,k}\gamma}{\langle f \rangle} & \dfrac{\psi_{2,k}\lambda}{\langle f \rangle} \end{bmatrix}.$$

The remaining variables satisfy the following differential equations:

$$\dot{S}_k(t) = -S_k(t)y_k(t) = -u_k(t), \tag{3.6}$$

$$\dot{R}_k(t) = Ex^{[k]}(t) = [\sigma\ \mu]x^{[k]}(t). \tag{3.7}$$

The overall infection-stage networked system is described by:

$$\dot{x} = (\mathbb{I}_N \otimes F)x + (\mathbb{I}_N \otimes b)\mathrm{diag}(S)cPx, \tag{3.8}$$

$$\dot{S} = -\mathrm{diag}(S)cPx, \tag{3.9}$$

where $x = [x_1^\top\ x_2^\top\ \cdots\ x_N^\top]^\top \in \mathbb{R}_+^{2N}$ where $\mathbb{R}_+^{2N}$ is the nonnegative orthant in $\mathbb{R}^{2N}$, $c = [c_1^\top\ c_2^\top\ \cdots\ c_N^\top]^\top \in \mathbb{R}_+^{2\times N}$, $S = [S_1\ S_2\ \cdots\ S_N]^\top \in \mathbb{R}_+^N$,

$$P = \frac{1}{\langle f \rangle}[n(1)P(1)\mathbb{I}_2\ n(2)P(2)\mathbb{I}_2 \cdots n(N)P(N)\mathbb{I}_2] \in \mathbb{R}_+^{2\times 2N},$$

where $\mathbb{I}_N$ is the $N \times N$ identity matrix, $\mathrm{diag}(S)$ is the diagonal matrix whose diagonal consists of $S_1, S_2, \ldots, S_N$, and $A \otimes B$ is the Kronecker product between matrix A and matrix B. The removed state is defined as in the following:

$$\dot{R} = (\mathbb{I}_N \otimes E)x, \tag{3.10}$$

where $R = [R_1 \ R_2 \ \cdots \ R_N]^\top$.

The transfer matrix of the positive system from vector $u = [u_1 \ u_2 \ \cdots \ u_N]^\top$ to vector $y = [y_1 \ y_2 \ \cdots \ y_N]^\top$ at zero frequency is the so-called networked basic reproduction matrix and it turns out to be the following:

$$\mathcal{R}_{0,net} = \frac{1}{\langle f \rangle} \begin{bmatrix} \mathcal{R}_{0,1} \\ \mathcal{R}_{0,2} \\ \vdots \\ \mathcal{R}_{0,N} \end{bmatrix} \begin{bmatrix} n(1)P(1) & n(2)P(2) & \cdots & n(N)P(N) \end{bmatrix} \in \mathbb{R}_+^{N \times N},$$

where $\mathcal{R}_{0,k}$ are the local basic reproduction number for every subsystem k, i.e.

$$\mathcal{R}_{0,k} = \frac{\psi_{1,k}\gamma\mu + \psi_{2,k}\lambda\alpha}{(\alpha+\sigma)\mu}.$$

For constant $\bar{S}$, the system is a feedback multivariable positive linear system, whose stability is equivalent to $\mathcal{R}_{0,net}\mathrm{diag}(\bar{S})$ being contractive, i.e.

$$\frac{1}{\langle f \rangle} \sum_{k=1}^{N} \mathcal{R}_{0,k} n(k) P(k) \bar{S}_k < 1.$$

Similarly to the homogeneous case, we provide a calculation of the nonzero epidemic threshold in the case of structured environment. Without loss of generality, let us consider system (3.1) with the following initial conditions, identical for all classes k: $R_k(0) = 0$ and $S_k(0) \simeq 1$, for which $A_k(0) = I_k(0) \simeq 0$. We find an expression for the epidemic threshold in the case of complex networks based on the spectral radius of $\mathcal{R}_{0,net}$, i.e.

$$\rho(\mathcal{R}_{0,net}) = \frac{1}{\langle f \rangle} \sum_{k=1}^{N} \mathcal{R}_{0,k} n(k) P(k).$$

When this value is less than 1, we are in the situation where the virus does not become an epidemic and instead wears off at the start.

THEOREM 3.1. *Consider system (3.1) with initial conditions $R_k(0) = 0$, $A_k(0) = I_k(0) \simeq 0$, $S_k(0) \simeq 1$. This system admits a nonzero epidemic prevalence if and only if*

$$\gamma > \gamma_c(1-p), \qquad \lambda > \lambda_c p,$$

for some $p \in [0\ 1]$, where γ_c and λ_c are the thresholds for the structured case and are defined as in the following:

$$\gamma_c \triangleq \frac{\langle f \rangle(\alpha+\sigma)}{\sum_{k=1}^{N} n(k)P(k)\psi_{1,k}}, \qquad \lambda_c \triangleq \frac{\langle f \rangle(\alpha+\sigma)\mu}{\alpha \sum_{k=1}^{N} n(k)P(k)\psi_{2,k}}. \tag{3.11}$$

Proof of Theorem 3.1. Consider the equation for $S_k(t)$ in system (3.1), by integrating it we have:

$$S_k(t) = S_k(0)e^{-c_k \frac{1}{\langle f \rangle} \sum_{j=1}^{N} n(j)P(j) \int_0^t x^{[j]}(\tau)\mathrm{d}\tau}.$$

From

$$\begin{bmatrix} \dot{I}_k \\ \dot{R}_k \end{bmatrix} = \begin{bmatrix} \alpha & -\mu \\ \sigma & \mu \end{bmatrix} x^{[k]},$$

we have

$$\begin{bmatrix} \mu & \mu \\ -\sigma & \alpha \end{bmatrix} \begin{bmatrix} I_k \\ R_k \end{bmatrix} = \int_0^t x^{[k]}(\tau)\mathrm{d}\tau.$$

By taking into account the initial conditions $S_k(0) \simeq 1$, $I_k(0) \simeq 0$ and $R_k(0) = 0$, we have

$$c_k \int_0^t x^{[j]}(\tau)\mathrm{d}\tau = \frac{\gamma\mu(I_j + R_j)\psi_{1,k} + (\alpha R_j - \sigma I_j)\psi_{2,k}\lambda}{\mu(\alpha + \lambda)},$$

and for $t \to \infty$

$$\begin{aligned} S_k(t) &= e^{-\frac{1}{\langle f \rangle} \sum_{j=1}^{N} n(j)P(j) \frac{\gamma\mu\psi_{1,k} + \alpha\lambda\psi_{2,k}}{\mu(\alpha+\lambda)} \bar{R}_j} \\ &= e^{-\frac{\mathcal{R}_{0,k}}{\langle f \rangle} \sum_{j=1}^{N} n(j)P(j)\bar{R}_j}, \end{aligned}$$

where the total number of infected for each class k is $\bar{R}_k = \lim_{t\to\infty} R_k(t)$ and $\mathcal{R}_{0,k}$ is the local basic reproduction number for subsystem k. We can now combine the above equation with the normalization condition and we can see that the total number of infected $\bar{R}_k$ fulfils the following equation:

$$\bar{R}_k = 1 - e^{-\frac{\mathcal{R}_{0,k}}{\langle f \rangle} \sum_{j=1}^{N} n(j)P(j)\bar{R}_j}.$$

We seek a nonzero solution for $\bar{R}_k$. As such, notice that:

$$\frac{\mathcal{R}_{0,k}}{\langle f \rangle} n(k)P(k) = \frac{\partial}{\partial \bar{R}_k} \left(1 - e^{-\frac{\mathcal{R}_{0,k}}{\langle f \rangle} \sum_{j=1}^{N} n(j)P(j)\bar{R}_j}\right)\Big|_{\bar{R}=0}.$$

When $\gamma > \gamma_c$ and $\lambda > \lambda_c$,

$$\frac{1}{\langle f \rangle} \sum_{k=1}^{N} \mathcal{R}_{0,k} n(k)P(k)\bar{S}_k \simeq \frac{1}{\langle f \rangle} \sum_{k=1}^{N} \mathcal{R}_{0,k} n(k)P(k) > 1 - p + p = 1.$$

Conversely, when $\frac{1}{\langle f \rangle} \sum_{k=1}^{N} \mathcal{R}_{0,k} n(k)P(k) > 1$ there exists p such that $\gamma > \gamma_c(1-p)$ and $\lambda > \lambda_c p$. This concludes the proof. ■

We now investigate the stability and convergence properties of the networked system. Analogously to the homogeneous case, we first consider constant parameters after time $\bar{t} = 0$.

THEOREM 3.2. *Assume that the parameters in F and c are constant for $t \geq 0$. Then,*

$$\log\frac{S_k(0)}{S_k(t)} - \frac{\mathcal{R}_{0,k}}{\langle f\rangle}\sum_{j=1}^{N} n(j)P(j)(S_j(0)-S_j(t)) \tag{3.12}$$

$$= \frac{\mathcal{R}_{0,k}}{\langle f\rangle}\sum_{j=1}^{N} n(j)P(j)(A_j(0)-A_j(t)) + \frac{1}{\langle f\rangle}\frac{\psi_{2,k}\lambda}{\mu}\sum_{j=1}^{N} n(j)P(j)(I_j(0)-I_j(t)),$$

$$\lim_{t\to\infty} A_k(t) = 0, \quad \forall k = 1,\dots,N, \tag{3.13}$$

$$\lim_{t\to\infty} I_k(t) = 0, \quad \forall k = 1,\dots,N, \tag{3.14}$$

$$\lim_{t\to\infty} S_k(t) = \bar{S}_k, \quad \forall k = 1,\dots,N, \tag{3.15}$$

where $\bar{S}_k$ are such that $\frac{1}{\langle f\rangle}\sum_{k=1}^{N} n(k)P(k)\bar{S}_k\mathcal{R}_{0,k} < 1$ and $\bar{S}$ is the only solution of

$$\log\frac{S_k(0)}{\bar{S}_k} - \frac{\mathcal{R}_{0,k}}{\langle f\rangle}\sum_{j=1}^{N} n(j)P(j)(S_j(0)-\bar{S}_j) \tag{3.16}$$

$$= \frac{\mathcal{R}_{0,k}}{\langle f\rangle}\sum_{j=1}^{N} n(j)P(j)A_j(0) + \frac{1}{\langle f\rangle}\frac{\psi_{2,k}\lambda}{\mu}\sum_{j=1}^{N} n(j)P(j)I_j(0).$$

Finally,

$$\bar{R}_k = \lim_{t\to\infty} R_k(t) = 1 - \bar{S}_k. \tag{3.17}$$

Proof of Theorem 3.2. In the following, recall that $x^{[j]} = [A_j\ I_j]^\top$. The first condition (3.12) comes from integrating $\dot{x} = (\mathbb{I}_N \otimes F)x + (\mathbb{I}_N \otimes b)\mathrm{diag}(S)cPx = (\mathbb{I}_N \otimes F)x - (\mathbb{I}_N \otimes b)\dot{S}$ and taking into account that $\dot{S}/S = -cx$ (element-wise). Consider now the Lyapunov function

$$V(x,S) = \mathbf{1}_{2N}^\top x + \mathbf{1}_N^\top(S-\bar{S}), \tag{3.18}$$

and take the derivative along the trajectories of system (3.1). Since $\mathbf{1}^\top F = -E \ll 0$ we have that

$$\dot{V}(x,S) = \mathbf{1}_{2N}^\top(\mathbb{I}_N \otimes F + (\mathbb{I}_N \otimes b)\mathrm{diag}(S)cP)x + \mathbf{1}_N^\top\dot{S}$$

$$= \mathbf{1}_{2N}^\top(\mathbb{I}_N \otimes F)x = -E\sum_{j=1}^{N} x^{[j]} < 0, \qquad x \neq 0.$$

This means that $x_k \to 0$, and therefore this justifies claims (3.13)-(3.14), and $S_k \to \bar{S}_k$ for a nonnegative $\bar{S}_k$. Therefore, (3.16) follows from (3.12) because of claims (3.13)-(3.14). The left-hand-side of (3.16) (element-wise) can be compactly rewritten as

$$\log\frac{S(0)}{\bar{S}} - \mathcal{R}_{0,net}(S(0)-\bar{S}),$$

whose gradient with respect $\bar{S}$ is matrix $-\mathrm{diag}(\bar{S})^{-1} + \mathcal{R}_{0,net}$. Since all S_k are decreasing, it follows that $-\mathrm{diag}(\bar{S})^{-1} + \mathcal{R}_{0,net} < 0$. This means $\frac{1}{\langle f\rangle}\sum_{k=1}^{N} n(k)P(k)\bar{S}_k\mathcal{R}_{0,k} < 1$. The proof of (3.17) is trivial. ∎

Remark. The above result provides the calculation of the equilibrium point of each subsystem k when the parameters and an initial condition for the subsystem are given. It can be seen as the extension of Theorem 2.3 to the heterogeneous case of a set of interlinked subsystems: when all subsystems have the same basic reproduction number, same distribution and the mean is equal to 1, we return to the homogeneous case. Analogously to Theorem 2.3, this result can be extended to any $t > 0$, provided that the parameters are known and the initial condition is replaced with the current values for each compartment at time $t > 0$.

The linear part $\dot{x} = (\mathbb{I}_N \otimes F)x$ is robustly stable under uncertain time-varying parameters in F. This important property implies convergence of the infection state variables of the nonlinear feedback system, namely $A_k(t)$ and $I_k(t)$, to zero for all k for any (bounded) time-varying parameters in F and c.

THEOREM 3.3. *The nonlinear feedback system (3.8)-(3.9) is exponentially convergent to $\bar{A} = 0$, $\bar{I} = 0$ and some constant vector $\bar{S} \geq 0$ that depends on the time-evolution of the parameters.*

Proof of Theorem 3.3. The linear system $\dot{x} = (I \otimes F)x$ is robustly stable with the common copositive linear Lyapunov function $\mathbf{1}_{2N}^\top x$, since $\mathbf{1}_{2N}^\top (I \otimes F)x = -E \sum_{j=1}^N x^{[j]} < 0$, $x \neq 0$, for any bounded time-varying parameters in F. Consider now the function

$$V(x, S) = \mathbf{1}_{2N}^\top x + \mathbf{1}_N^\top S.$$

Therefore,

$$\begin{aligned} \dot{V} &= \mathbf{1}_{2N}^\top (\mathbb{I}_N \otimes F + (\mathbb{I}_N \otimes b)\mathrm{diag}(S)cP)x + \mathbf{1}_N^\top \dot{S} \\ &= \mathbf{1}_{2N}^\top (\mathbb{I}_N \otimes F)x = -E \sum_{j=1}^N x^{[j]} < 0, \qquad x \neq 0. \end{aligned}$$

Therefore x converges to 0 and from $\dot{S} \leq 0$, S converges to a constant $\bar{S}$ that depends of the time-varying parameters in F and c. This concludes the proof. ■

Remark. The above result extends the results obtained in the homogeneous case to the structured case. In this setting, parameters $\bar{\psi}_{1,k} \leq 1$ and $\bar{\psi}_{2,k}$ reflect the lower connectivity in the population as a result of the NPIs (non-pharmaceutical interventions) that are different within each class of connectivity k. In the homogeneous case, the parameters $\bar{k}_1$ and $\bar{k}_2$ are the same for the whole population, whereas we can see the heterogeneous case as a multi-population scenario with different parameters $\bar{\psi}_{1,k} \leq 1$ and $\bar{\psi}_{2,k}$. These classes can be seen as a local area or region.

We end this section by investigating the ratio between infected and asymptomatic individuals for all classes of connectivity, in a similar manner as for the homogeneous system. To this end, let $\tilde{I}_k := I_k/A_k$, and let us define the coupling between class j and k as $v_{jk} := A_j/A_k$. Therefore we have the following system of cross-coupled Riccati equations:

$$\begin{cases} \dot{\tilde{I}}_k = \alpha - \mu \tilde{I}_k + S_k(\alpha + \sigma)\tilde{I}_k - S_k \tilde{I}_k Z_k, \\ \dot{v}_{jk} = (S_j - v_{jk} S_k) Z_k, \quad for j \neq k, \\ Z_k = \frac{1}{\langle f \rangle}\Big[\psi_{1,k}\gamma \sum_{j=1}^N n(j)P(j)v_{jk} + \psi_{2,k}\lambda \sum_{j=1}^N n(j)P(j)v_{jk}\tilde{I}_j\Big]. \end{cases} \tag{3.19}$$

The following result is straightforward and therefore it is stated without proof.

THEOREM 3.4. *Given* $\bar{S}_1, \ldots, \bar{S}_N$ *as in Theorem 3.2, it holds* $\bar{v}_{jk} = \bar{S}_j/\bar{S}_k$ *at steady state and system (3.19) converges to the equilibrium*

$$\bar{\bar{I}}_k = \frac{\alpha}{\mu - \bar{S}_k(\alpha+\sigma) + \bar{S}_k\bar{Z}_k}, \tag{3.20}$$

$$\bar{S}_k\bar{Z}_k\langle f\rangle = \sum_{j=1}^{N} n(j)P(j)\bar{S}_j(\psi_{1,k}\gamma + \psi_{2,k}\lambda\bar{\bar{I}}_j), \tag{3.21}$$

which is asymptotically stable.

4. Numerical Analysis. In this section, we present the numerical analysis conducted on the Watts-Strogatz model to show the impact of heterogeneous connectivity in system (3.1). For the purpose of illustration, we consider a WS model for $N = 1000$ nodes, given $\langle f\rangle = 2m$ and $m = 4$. To generate the network we use a discretized version of the formula $P(k) = m^{(k-m)}/((k-m)!e^{-m})$, for $k \geq m$, where the node degrees vary between 4 and 14. The discretized version is obtained from discarding the values less than 4 and greater than 14, and rounding up the fractions of the populations in the other classes such that the total population across the classes sums up to 1. We also set $p = 1$, where p is the probability of rewiring a node from the starting ring graph, each node being connected to its $2m$ nearest neighbors [34]. Figure 4 shows the corresponding WS complex network, where the colour of each node corresponds to its node degree as in the colorbar on the right.

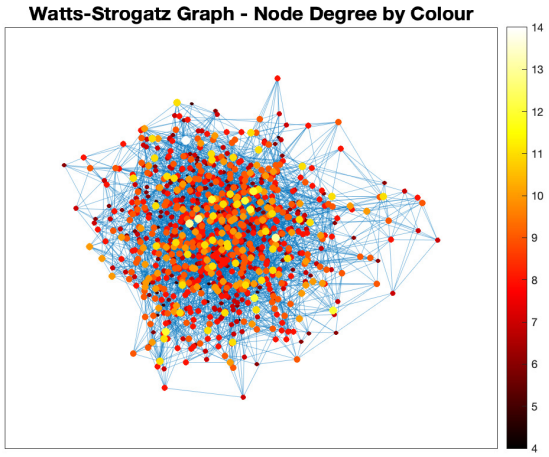

Fig. 4: Small world network with $N = 1000$, $m = 4$ and $p = 1$, where the colour of each node corresponds to its node degree as in the colorbar.

4.1. Parameter Estimation. In this section, we discuss the algorithm that we used to estimate the parameters of the homogeneous model in (2.1). It consists of an adaptation of the widely used nonlinear least squares minimization algorithm under the set of constraints coming from the physical interpretation that we have provided for these parameters after (2.1). The objective of the least squares optimization problem is to estimate the values of the parameters of infection indicated by lowercase

Greek letters, namely γ, λ, α, σ and μ, and the parameters of interaction indicated by $\bar{k}_1$ and $\bar{k}_2$ to best fit the official data. We assume that the parameters of infection are constant throughout the entire time window and that the only parameters that change are k_1 and k_2, which represent the average number of contacts per unit time of susceptible with asymptomatic and with symptomatic infected, respectively.

One of the crucial aspect of the parameter estimation is the way in which we treat $\bar{k}_1$ and $\bar{k}_2$. As previously mentioned, they are the only parameters that we update in relation to the policy-making from the government. A sensible approach is to model these two values through a logarithmic function with given constraints: at the beginning and during the whole time window $\bar{k}_1 > \bar{k}_2$, as it is more likely to get in contact with an asymptomatic individual than with a symptomatic one; these values vary between 0 and 1, and the value represents the average number of interactions within your network (1 being interacting with all your network as normal and 0 with nobody). We give a physical interpretation on this choice: these parameters represent the change in social habits before and after the lockdown and similar NPIs. We use the following function to model the evolution of $\bar{k}_i$: $\bar{k}_i = (k_i^0 - k_i^T)/(1 + e^{-C(-t+LD+LO)} + k_i^T)$, for $i = 1, 2$, where k_i^0 is the initial value of $\bar{k}_i$, $k_i^T = 0.9k_i^0$ is the final value where 0.9 is a decreasing factor, C is a constant that measure the abruptness of the change, LD is the lockdown date and LO is an offset to the lockdown date. The motivation to use this function can be explained as, although the lockdown significantly alters the behavior of the population, the change is smooth over a few days and the tangible effects are delayed.

We are now ready to present our algorithm, as illustrated in Table 1. Our algorithm is designed to fit the official data and estimate the parameters of our model. It extends an implementation of the non-linear least squares regression built in the python library *LMFIT*, see [35] and [36]. In particular, we used an implementation of a non-linear least squares regression, using the Levenberg-Marquardt algorithm [37]. This is an iterative optimization algorithm that fits a function to a desired output, obtaining the parameters that minimize the square error between the output of the function and the objective value given. In this specific case, the values that were fit were the number of symptomatic active cases and the number of removed. This algorithm is widely used because of its versatility and efficient use of data, even on small datasets [38]. However, it is very sensitive to the hyperparameters so an educated initial estimation of them was done based on [13] as well as the specific range of values that each parameter could take. These parameter values, which were analytically extracted, were used as a starting point, and were later adapted to better match the official data, especially for the heterogeneous case. A comprehensive review of the identifiability and observability of the parameters in COVID-19 data driven models has been conducted in [39]. In the heterogeneous case, a network structure based on the density of the population in each region is assumed; however, we refer the reader to [40] for a study on the network reconstruction in the context of epidemic outbreaks.

5. Case Study. In this section, we propose a case study where we use the official data from Dipartimento della Protezione Civile [41, 42], and also we provide an investigation on the impact of asymptomatic infected through the recent seroprevalence study conducted by Istat [31]. We provide two case studies, the first one uses the homogeneous model and the second uses the heterogeneous model. The first case study includes two sets of simulations: in the first one, we use the official data to estimate the parameters of our model and study the difference between the data and the estimated number of individuals with antibodies found in the seroprevalence study;

Table 1: Algorithm used to estimate the parameters of the homogeneous model.

Algorithm

Input: Official data, model initial states and initial guess of the parameters.
Output: Estimation of the parameters in *param*.

Initialization:
Initialize the parameters and the model.
data: infected data **concat** removed data.
param: γ, λ, α, σ, μ, $\bar{k}_i$.
Function **Increasing**(y, t, *param*):
$\mathrm{d}S(t)/\mathrm{d}t = -S(t)(\gamma\bar{k}_1 A(t) + \lambda\bar{k}_2 I(t))$,
$\mathrm{d}A(t)/\mathrm{d}t = S(t)(\gamma\bar{k}_1 A(t) + \lambda\bar{k}_2 I(t)) - A(t)(\alpha+\sigma)$,
$\mathrm{d}I(t)/\mathrm{d}t = A(t)\alpha - I(t)\mu$,
$\mathrm{d}R(t)/\mathrm{d}t = A(t)\sigma + I(t)\mu$.
return $\mathrm{d}S(t), \mathrm{d}A(t), \mathrm{d}I(t), \mathrm{d}R(t)$.
Function **Model**(y, *param*):
for $t = 1 : T$
$y(t) = y(t-1)+$ Increasing(y, t, *param*)
end
return $y.I[0\ T]$ **concat** $y.R[0\ T]$
return
Minimize LSE(Model(y, t, *param*), *data*)
STOP

in the second one, we do the opposite, i.e. we fit our model with the seroprevalence study and compare our model to the official data. In the second case study, we investigate the interactions across different regions in Italy and provide a prediction on the evolution of the pandemic for two specific regions, Lombardy and Campania, over the first weeks of September in the context of school opening.

5.1. Homogeneous Model: Data and Seroprevalence Study. In the first investigation, we use the official data to fit our model and estimate the parameters and then we compare our model to the value of the Istat seroprevalence study. We set the portion of the population in each stage as: $A(0) = 94/(60{*}10^6)$, $I(0) = 127/(60{*}10^6)$, $R(0) = 0$, and $S(0) = 1-A(0)-I(0)-R(0)$, where these values are taken from the data for the isolated at home and hospitalized infected [42]. The reason behind this choice is that we believe that people that are not hospitalized must either be asymptomatic or paucisymptomatic and thus would fall in our category of asymptomatic infected. The parameters being learnt by the least squares optimization problem stated in the previous section are the ones as in the following: $\gamma = 0.46952$, $\sigma = 0.025501$, $\bar{k}_1 = 0.99209$, $\lambda = 0.48521$, $\mu = 0.10004$, $\bar{k}_2 = 0.65056$, $\alpha = 0.185017$. Due to the similar viral load between symptomatic and asymptomatic individuals [16], we set the values of γ and λ to be very close. Parameter $\bar{k}_1$ is chosen to be larger than $\bar{k}_2$ at the start (and also in future time instants), because it accounts for the likelihood that people interact with asymptomatic individuals more likely than with infected that show symptoms. On March 6th, prime minister Giuseppe Conte imposed a set of localized lockdowns to isolate the outbreaks, and on March 9th a national quarantine

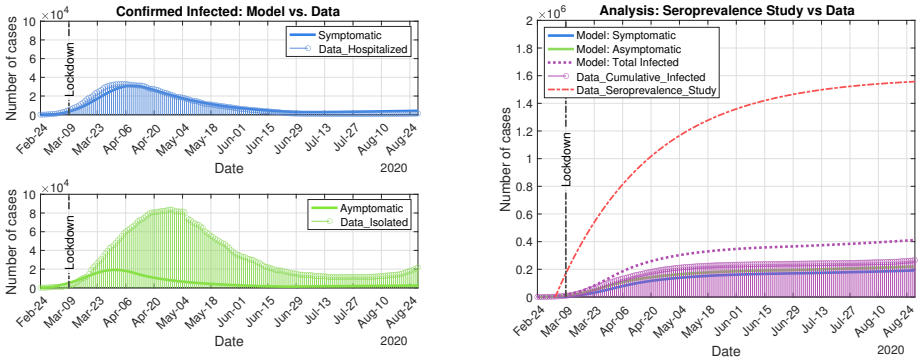

Fig. 5: Model vs. data: the symptomatic and asymptomatic classes in the model are plotted against hospitalized and isolated data from [42] (left). Analysis: symptomatic and asymptomatic classes in the model vs the prediction from the Istat seroprevalence study [31] vs the official data from [42] (right).

was imposed, which restricted the movements of the population and therefore their contacts and interactions. We account for this by lowering the values of $\bar{k}_1$ and $\bar{k}_2$ slowly over the days following the lockdown, down to $\bar{k}_1 = 0.2957$ and $\bar{k}_2 = 0.0305$ before the end of the quarantine period. Following the ease of the lockdown measures, we set $\bar{k}_1 = 0.3636$ and $\bar{k}_2 = 0.0594$ to account for the increased interactions during mid-August holidays. At the end of February and thus before the lockdown, we estimate $\mathcal{R}_0 = 4.98$, in accordance with studies that place it between 2 and 5 [43–46], depending on the estimation of the number of asymptomatic cases. Towards the end of the quarantine, the value of $\mathcal{R}_0$ goes below 1 and then it oscillates around $\mathcal{R}_0 = 1.06$ during August. As it can be seen in Fig. 5 (left), our model matches quite accurately the recovered and hospitalized infected, but it does not do the same with the asymptomatic infected. Even in that case, we can see from Fig. 5 (right) that our estimation of the cumulative infected is higher that the confirmed cases. It is matching quite closely an early estimate of the undetected asymptomatic being around 30%, but far from the current Istat estimate depicted in red.

In the second investigation, we use the seroprevalence study to fit our model and estimate the parameters. We set the initial conditions as in the previous investigation. This time, the parameters being learnt are set as in the following: $\gamma = 0.46952$, $\sigma = 0.065501$, $\bar{k}_1 = 0.99209$, $\lambda = 0.48521$, $\mu = 0.15004$, $\bar{k}_2 = 0.65056$, $\alpha = 0.050017$. During the days following the local and national quarantine, we lower the values of $\bar{k}_1$ and $\bar{k}_2$ to 0.1916 and 0.0478, respectively, and then we account for the increased connectivity during August by setting them to $\bar{k}_1 = 0.2738$ and $\bar{k}_2 = 0.0971$. The basic reproduction number is calculated as $\mathcal{R}_0 = 4.9432$ at the beginning of the pandemic, and $\mathcal{R}_0 = 1.2490$ at the end of August. As it can be seen in Fig. 6 (left), our model matches with the hospitalized infected accurately, but it suggests a higher number of asymptomatic to balance for matching the value of the seroprevalence study. As it is done in the previous case, we interpolate the value of the seroprevalence study by using an exponential regression as depicted in red in Fig. 6 (right). We chose the parameters such that our estimation of the cumulative infected, i.e. the purple dotted curve, matches the predicted infected from the seroprevalence study. By taking into account the seroprevalence study, we first calculate the value of $\bar{\bar{I}} = 0.2876$ in accordance

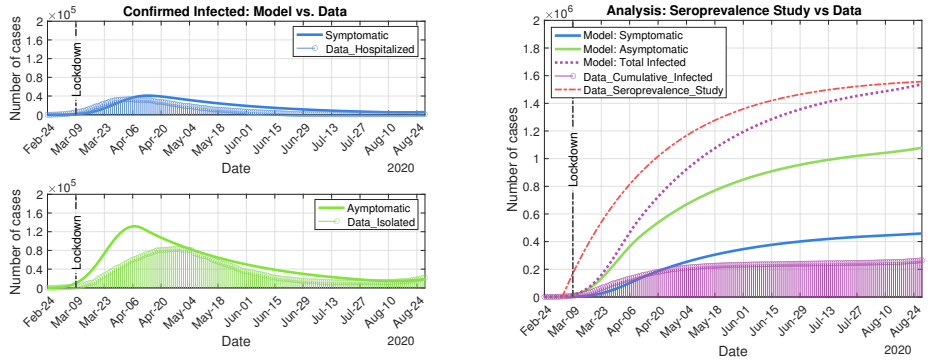

Fig. 6: Model vs data: the symptomatic and asymptomatic classes in the model are plotted against hospitalized and isolated data from [42] (left). Analysis: symptomatic and asymptomatic classes in the model vs the prediction from the Istat seroprevalence study [31] vs the official data from [42].

with Theorem 2.5, and this value is identical to the one obtained at the end of our simulation. We explicitly calculate the total number of people that have contracted the disease through our model by subtracting the confirmed deaths from the Removed state. We estimate a total of $8.48 * 10^5$ individuals who contracted the disease and are currently healthy. When using the work of Böhning *et al.* to estimate the hidden infection, we obtain a different value of hidden infections, namely 264240 [47]. This value would account for twice as many infected individuals as the number of detected infections, but it is underestimated if compared with seroprevalence studies [31,48]. A high percentage of individuals (estimated around 90%) remained undetected because these individuals did not show symptoms. This large value is in accordance with what was reported in the following months, namely October and November, with an increased number of tests performed.

5.2. Complex Networks: Model vs Data. Now, we use the proposed structured model, namely system (3.1), to discuss the impact of increased interactions in the population corresponding to school opening in September and to the effects of increased tourism during August, especially in the southern regions. We set the initial conditions as in the data [42], where we take the regional data and set different parameters of connectivity $\psi_{1,k}$ and $\psi_{2,k}$ depending on the region and the corresponding exposure to the virus in Italy. As before, we set the general parameters of the model as $\gamma = 0.49952,\ \sigma = 0.05050, \alpha = 0.03351,\ \lambda = 0.59952,\ \mu = 0.15044$. The population in each class is split according to a similar discretized version of the Watts-Strogatz network as the one used in the numerical analysis (Section 4). The distribution corresponding to each region is equal to portion of the actual population of that region in Italy as in the following: Abruzzo 0.022, Basilicata 0.009, Calabria 0.032, Campania 0.096, Emilia-Romagna 0.073, Friuli-Venezia Giulia 0.02, Lazio 0.098, Liguria 0.026, Lombardy 0.166, Marche 0.025, Molise 0.005, A.P. Bolzano 0.009, A.P. Trento 0.009, Piedmont 0.072, Apulia 0.068, Sardinia 0.027, Sicily 0.083, Tuscany 0.062, Umbria 0.015, Aosta Valley 0.002 and Veneto 0.081.

As in the previous case study, we gradually lower the values of $\psi_{1,k}$ and $\psi_{2,k}$ around the lockdown date and the following few days in an identical manner for all

regions. Then, we fit our model with the data until October 7th. We start raising the connectivity values in correspondence of early August to account for an increased number of tourists in a way that considers a larger incidence for southern regions. We increase these values further in correspondence to the opening of schools in mid-September to account for secondary infections (which are very limited as reported by ISS). It is worth noting that the increase is proportional to the value of $\psi_{1,k}$ and $\psi_{2,k}$, namely we increase these parameters by a percentage of their actual value at time t, more for the southern regions to reflect what has been discussed before. Therefore, regions with a higher connectivity (taken from fitting the model to the data) would have a higher increase. As shown in Fig. 7, our model captures the evolution of the cumulative infected for all regions with an error of 1%-3%. It is worth noting that this multi-population scenario is very difficult to fit with the data as we consider a general interaction model instead of a selective one, in the sense that individuals in one region interact with individuals in other regions by means of θ_1 and θ_2. The increase in social interactions, and thus the parameters of connectivity in our model, because of the summer holidays and return to school would explain the start of the second wave in Europe and specifically in Italy. In accordance with Theorem 3.4, we can calculate the value of $\tilde{\bar{I}}_k$ for each class k, and we can see that it takes values between 0.2229 and 0.2713, similarly to the homogeneous case. With the given parameters, we also calculate the $\bar{S}_k$ and can estimate that without any other NPIs or vaccinations most of the population would become infected. Our model would therefore support the need for NPIs until the vaccination campaign can ensure the attainment of the herd immunity.

Finally, we use the official data up to October, 7th, to highlight the impact of tourism and of the return to school in a region in the north, i.e. Lombardy, and in a region in the south, i.e. Campania. On account of these two aspects, we model the parameters $\psi_{1,k}$ and $\psi_{2,k}$ asymmetrically, meaning that for Campania the values are increasing twice as much as for Lombardy. Figure 8 depicts the evolution of system (3.1) for these two regions. Despite the lower number of cases in early August, the number of infections in Campania is dramatically increasing due to the large amount of tourists during summer, and possibly also due to the less adherence to the policies. In Lombardy, the situation is different: although the number of cases is increasing slowly but steadily, the curve is almost flat. We have also estimated the effective reproductive number $\mathcal{R}_t$ for both regions, and this is depicted in the top-right box for each figure. It is interesting to note that while the value of $\mathcal{R}_t$ is almost stable in the case of Lombardy, and it is slightly above 1, the situation in Campania is more worrying, as higher peaks are present between September and October.

Our case study provides two clear messages. When we use the Istat seroprevalence study and fit our model with the official data, we can see a plausible evolution of the number of cumulative infected in the early stages of the pandemic. The number of asymptomatic is clearly underestimated in the official data and their role is crucial in that they can undermine the stability of the system and force another wave. This is even more true in recent times, where the vast majority of new infections are younger individuals who rarely manifest symptoms (currently the estimate of asymptomatic infections is around 95% of the total). When we look at the regional level, our work shows the need to keep our guard up at all times. Southern regions in Italy have been experiencing a massive increase in new cases, despite the relatively low numbers at the beginning of August. This can be linked to the impact of the asymptomatic cases because of the higher number of social interactions due to tourism (much more

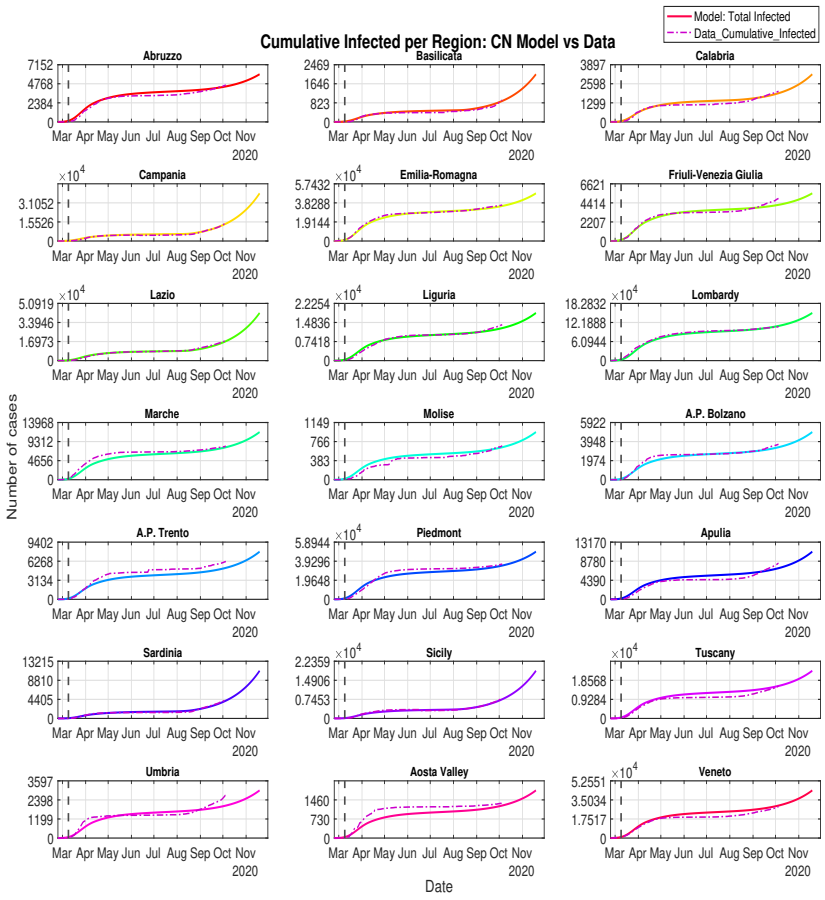

Fig. 7: Total cumulative infected: heterogeneous model vs regional data [31]. We increase the parameters of connectivity over the time window that corresponds to the holidays (mid-August) and the return to school (mid-September).

extensive in the southern regions during summer) and return to school.

6. Conclusion. In this paper, we have studied an epidemic model, which we called SAIR, as a compartmental discrete-state continuous-time system. We have studied the equilibrium and stability of the homogeneous system in feedback form in terms of the basic reproduction number $\mathcal{R}_0$ and discussed the corresponding epidemic threshold above which the virus propagates and becomes an epidemic. Additionally, we have investigated the role of asymptomatic infections through the ratio between symptomatic and asymptomatic infected in the population. We have extended our analysis to the structured case, where the structure is captured by a complex network. Also in this case, we have carried out the stability analysis of each subsystem and of the whole system for all classes of connectivity. We have found the corresponding expression of the epidemic threshold in the structured case. Finally, we

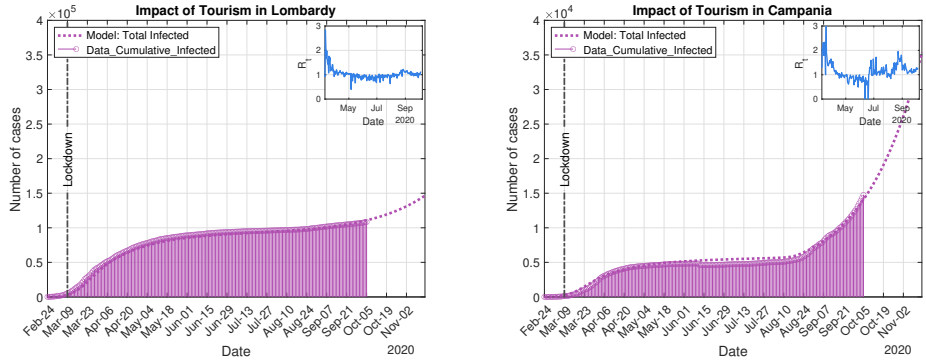

Fig. 8: Propagation of the disease on account of tourism and estimate of the effective reproduction number $\mathcal{R}_t$ in Lombardy (left) and in Campania (right).

have presented a case study for the situation in Italy, analyzing the homogeneous and heterogeneous cases and the impact of tourism and schools via the structured model. Our study highlights the relevance of heterogeneous interactions in spreading SARS-CoV-2 while emphasizing the threat of asymptomatic individuals yet not detected and therefore not being isolated. In the asymptomatic category, our model includes those individuals that do not have symptoms or are paucisymptomatic. The Istat seroprevalence study, as well as official data from Protezione Civile, for the propagation of COVID-19 in Italy guided our data-driven modelling approach. Future works include the data analysis and parameter estimation in the networked case, the study of the corresponding Markovian dynamics via numerical simulations, as well as the extension to the Barabási-Albert and Erdős-Rényi models.

Data Sources. The data used in this manuscript were downloaded on 31 August 2020 for all figures. Policy decisions based upon models fit to these data must take these ascertainment and data quality issues into account. The code used to generate all figures can be downloaded from GitHub at: https://github.com/lleonardostella/SAIR

Acknowledgements. This research was partly supported by the Early Career Researchers Development Fund, University of Derby.

REFERENCES

[1] J. D. Mathews, C.T. McCaw, J. McVernon, E.S. McBryde and J.M. McCaw, "A biological model for influenza transmission: pandemic planning implications of asymptomatic infection and immunity", *PLoS ONE*, 2007.

[2] M. Robinson and N. Stilianakis, "A model for the emergence of drug resistance in the presence of asymptomatic infections", *Mathematical Biosciences*, vol. 243, no. 2, pp. 163-177, 2013. Available: 10.1016/j.mbs.2013.03.003.

[3] S. Ansumali, S. Kaushal, A. Kumar, M. Prakash and M. Vidyasagar, "Modelling a pandemic with asymptomatic patients, impact of lockdown and herd immunity, with applications to SARS-CoV-2", *Annual Reviews in Control*, vol. 50, pp. 432-447, 2020. Available: 10.1016/j.arcontrol.2020.10.003.

[4] N. Zhu *et al.*, "A novel coronavirus from patients with pneumonia in China, 2019", *New England Journal of Medicine*, vol. 382, no. 8, pp. 727-733, 2020. Available: 10.1056/NEJMoa2001017.

[5] R. M. Anderson and R. M. May, *Infectious diseases of humans*. Oxford: Oxford Univ. Press, 1992.

[6] H. Hethcote, "The Mathematics of Infectious Diseases", *SIAM Review*, vol. 42, no. 4, pp. 599-653, 2000. Available: 10.1137/s0036144500371907.

[7] W. O. Kermack and A. G. McKendrick, "A Contribution to the Mathematical Theory of Epidemics", in *Proceedings of the Royal Society of London A*, vol. 115, no. 772, pp. 700-721, 1927. Available: doi:10.1098/rspa.1927.0118.

[8] A. B. Gumel, S. Ruan, T. Day *et al.*, "Modelling strategies for controlling SARS outbreaks", *Proceedings of the Royal Society of London. Series B: Biological Sciences*, vol. 271, no. 1554, pp. 2223-2232, 2004. Available: 10.1098/rspb.2004.2800.

[9] R. M. May and R. M. Anderson, "The transmission dynamics of human immunodeficiency virus (HIV)", *Philosophical Transactions of the Royal Society of London. B, Biological Sciences*, vol. 321, no. 1207, pp. 565-607, 1988. Available: 10.1098/rstb.1988.0108.

[10] B. Korber, W. M. Fischer, S. Gnanakaran *et al.*, "Spike mutation pipeline reveals the emergence of a more transmissible form of SARS-CoV-2", *bioRxiv*, 2020. Available: 10.1101/2020.04.29.069054.

[11] J. Liu, P. Pare, A. Nedic *et al.*, "Analysis and Control of a Continuous-Time Bi-Virus Model", *IEEE Transactions on Automatic Control*, vol. 64, no. 12, pp. 4891-4906, 2019. Available: 10.1109/tac.2019.2898515.

[12] Z. Zhang and E. Enns, "Optimal Timing and Effectiveness of COVID-19 Outbreak Responses in China: A Modelling Study", *SSRN Electronic Journal*, 2020. Available: 10.2139/ssrn.3558339.

[13] G. Giordano, F. Blanchini, R. Bruno *et al.* "Modelling the Covid-19 Epidemic and Implementation of Population-Wide Interventions in Italy", *Nature Medicine*. Available: 10.1038/s41591-020-0883-7.

[14] G. Giordano, M. Colaneri, A. Di Filippo *et al.*, "Modeling Vaccination Rollouts, SARS-CoV-2 Variants and the Requirement for non-Pharmaceutical Interventions in Italy", *Nature Medicine*, 2021. Available: 10.1038/s41591-021-01334-5.

[15] Y. Wang, Y. Wang, Y. Chen and Q. Qin, "Unique epidemiological and clinical features of the emerging 2019 novel coronavirus pneumonia (COVID-19) implicate special control measures", *Journal of Medical Virology*, vol. 92, no. 6, pp. 568-576, 2020. Available: 10.1002/jmv.25748.

[16] L. Zou, F. Ruan, M. Huang *et al.*, "SARS-CoV-2 Viral Load in Upper Respiratory Specimens of Infected Patients", *New England Journal of Medicine*, vol. 382, no. 12, pp. 1177-1179, 2020. Available: 10.1056/nejmc2001737.

[17] C. Rothe, M. Schunk, P. Sothmann *et al.*, "Transmission of 2019-nCoV Infection from an Asymptomatic Contact in Germany", *New England Journal of Medicine*, vol. 382, no. 10, pp. 970-971, 2020. Available: 10.1056/nejmc2001468.

[18] A. Bertozzi, E. Franco, G. Mohler, M. Short and D. Sledge, "The challenges of modeling and forecasting the spread of COVID-19", *Proceedings of the National Academy of Sciences*, vol. 117, no. 29, pp. 16732-16738, 2020. Available: 10.1073/pnas.2006520117.

[19] F. Casella, "Can the COVID-19 Epidemic Be Controlled on the Basis of Daily Test Reports?", *IEEE Control Systems Letters*, vol. 5, no. 3, pp. 1079-1084, 2020. Available: 10.1109/lcsys.2020.3009912.

[20] F. Della Rossa et al., "A network model of Italy shows that intermittent regional strategies can alleviate the COVID-19 epidemic", *Nature Communications*, vol. 11, no. 1, 2020. Available: 10.1038/s41467-020-18827-5.

[21] S. Yilmaz, E. Dudkina, M. Bin *et al.*, "Kemeny-based testing for COVID-19", *PlosOne*, 2020. Available: 10.1371/journal.pone.0242401.

[22] E. Franco, "A feedback SIR (fSIR) model highlights advantages and limitations of infection-based social distancing", arXiv, 2020. Available: https://arxiv.org/abs/2004.13216.

[23] G. C. Calafiore, C. Novara, C. Possieri, "A Modified SIR Model for the COVID-19 Contagion in Italy", *Proceedings of the 59th IEEE Conference on Decision and Control (CDC)*, 2020. Available: 10.1109/CDC42340.2020.9304142.

[24] K. J. Friston, T. Parr, P. Zeidman *et al.*, "Testing and tracking in the UK: A dynamic causal modelling study", *Wellcome Open Research*, vol. 5, p. 144, 2020. Available: 10.12688/wellcomeopenres.16004.1.

[25] P. Garibaldi, E. R. Moen and C. A. Pissarides, "Modelling contacts and transitions in the SIR epidemics model", *Covid Economics*, no. 5, 2020. Available: https://www.carloalberto.org/wp-content/uploads/2020/04/garibaldi.pdf.

[26] R. Pastor-Satorras, C. Castellano, P. Van Mieghem and A. Vespignani, "Epidemic processes in complex networks", *Reviews of Modern Physics*, vol. 87, 2015.

[27] S. Tan, J. Lu, G. Chen and D. Hill, "When Structure Meets Function in Evolutionary Dynamics on Complex Networks", *IEEE Circuits and Systems Magazine*, vol. 14, no. 4, pp. 36-50,

2014. Available: 10.1109/mcas.2014.2360790.
[28] W. Mei, S. Mohagheghi, S. Zampieri and F. Bullo, "On the dynamics of deterministic epidemic propagation over networks", *Annual Reviews in Control*, vol. 44, pp. 116-128, 2017. Available: 10.1016/j.arcontrol.2017.09.002.
[29] Y. Moreno, R. Pastor-Satorras and A. Vespignani, "Epidemic outbreaks in complex heterogeneous networks", *The European Physical Journal B*, vol. 26, no. 4, pp. 521-529, 2002. Available: 10.1140/epjb/e20020122.
[30] R. Pastor-Satorras, C. Castellano, P. Van Mieghem and A. Vespignani, "Epidemic processes in complex networks", *Reviews of Modern Physics*, vol. 87, no. 3, pages 925-979, 2015. Available: 10.1103/RevModPhys.87.925.
[31] "Indagine sierologica su Covid-19 condotta da Ministero della Salute e Istat", *Istat.it*, 2020. [Online]. Available: https://www.istat.it/it/archivio/242676. [Accessed: 09-Aug-2020].
[32] M. D'Arienzo and A. Coniglio, "Assessment of the SARS-CoV-2 basic reproduction number, R0, based on the early phase of COVID-19 outbreak in Italy", *Biosafety and Health*, vol. 2, no. 2, pp. 57-59, 2020. Available: 10.1016/j.bsheal.2020.03.004.
[33] H. Maeda, S. Kodama and Y. Ohta, "Asymptotic behavior of nonlinear compartmental systems: Nonoscillation and stability", *IEEE Transactions on Circuits and Systems*, vol. 25, no. 6, pp. 372-378, 1978. Available: 10.1109/tcs.1978.1084490.
[34] A. Barrat and M. Weigt, "On the properties of small-world network models", *The European Physical Journal B*, vol. 13, no. 3, pp. 547-560, 2000. Available: 10.1007/s100510050067.
[35] K. Sasaki, "COVID-19 dynamics with SIR model", *The First Cry of Atom*, 2020. [Online]. Available: https://www.lewuathe.com/covid-19-dynamics-with-sir-model.html. [Accessed: 16-Jun-2020].
[36] H. Froese, "Infectious Disease Modelling: Understanding the models that are used to model Coronavirus", *towardsdatascience*, 2020. [Online]. Available: https://towardsdatascience.com/infectious-disease-modelling-part-i-understanding-sir-28d60e29fdfc. [Accessed: 16-Jun-2020].
[37] I. Griva, S. G. Nash and A. Sofer, *Linear And Nonlinear Optimization*. SIAM, 2008. ISBN: 978-0-898716-61-0
[38] NIST/SEMATECH, *E-Handbook Of Statistical Methods*, 2003. [online] Available: http://www.itl.nist.gov/div898/handbook/. [Accessed: 1-Sep-2020].
[39] G. Massonis, J. Banga and A. Villaverde, "Structural Identifiability and Observability of Compartmental Models of the COVID-19 Pandemic", *Annual Reviews in Control*, vol. 51, pp. 441-459, 2021. Available: 10.1016/j.arcontrol.2020.12.001.
[40] B. Prasse and P. Van Mieghem, "Network Reconstruction and Prediction of Epidemic Outbreaks for General Group-Based Compartmental Epidemic Models", *IEEE Transactions on Network Science and Engineering*, vol. 7, no. 4, pp. 2755-2764, 2020. Available: 10.1109/tnse.2020.2987771.
[41] "Dipartimento della Protezione Civile", *Dipartimento della Protezione Civile*, 2020. [Online]. Available: http://www.protezionecivile.gov.it/. [Accessed: 09-Aug-2020].
[42] "pcm-dpc/COVID-19", *GitHub*, 2020. [Online]. Available: https://github.com/pcm-dpc/COVID-19. [Accessed: 09-Aug-2020].
[43] J. Wu, K. Leung and G. Leung, "Nowcasting and forecasting the potential domestic and international spread of the 2019-nCoV outbreak originating in Wuhan, China: a modelling study", *The Lancet*, vol. 395, no. 10225, pp. 689-697, 2020. Available: 10.1016/s0140-6736(20)30260-9.
[44] S. Zhao, Q. Linc, J. Ran *et al.*, "Preliminary estimation of the basic reproduction number of novel coronavirus (2019-nCoV) in China, from 2019 to 2020: A data-driven analysis in the early phase of the outbreak", *International Journal of Infectious Diseases*, vol. 92, pp. 214-217, 2020. Available: 10.1016/j.ijid.2020.01.050.
[45] C. Anastassopoulou, L. Russo, A. Tsakris and C. Siettos, "Data-based analysis, modelling and forecasting of the COVID-19 outbreak", *PLOS ONE*, vol. 15, no. 3, p. e0230405, 2020. Available: 10.1371/journal.pone.0230405.
[46] M. Gatto *et al.*, "Spread and dynamics of the COVID-19 epidemic in Italy: Effects of emergency containment measures", *Proceedings of the National Academy of Sciences*, vol. 117, no. 19, pp. 10484-10491, 2020. Available: 10.1073/pnas.2004978117.
[47] D. Böhning, I. Rocchetti, A. Maruotti and H. Holling, "Estimating the undetected infections in the Covid-19 outbreak by harnessing capture-recapture methods", *International Journal of Infectious Diseases*, vol. 97, pp. 197-201, 2020. Available: 10.1016/j.ijid.2020.06.009.
[48] M. Pollan, B. Perez-Gomez, R. Pastor-Barriuso *et al.*, "Prevalence of SARS-CoV-2 in Spain (ENE-COVID): a nationwide, population-based seroepidemiological study". *The Lancet*, vol. 396, no. 10250, pp. 535-544, 2020. Available: 10.1016/S0140-6736(20)31483-5.